# Electron−Phonon Interactions in the Monoanions of Polycyanodienes

**Takashi Kato* and Tokio Yamabe**

*Institute for Innovative Science and Technology, Graduate School of Engineering, Nagasaki Institute of Applied Science, 3-1, Shuku-machi, Nagasaki 851-0121, Japan*

*Received: June 30, 2004*

The single charge transfer through cyanodienes is discussed. The reorganization energies between the neutral molecules and the corresponding monoanions for cyanodienes are larger than those for acenes with $D_{2h}$ geometry. This result implies that the negatively charged cyanodienes would not be better conductors with slow electron transfer than the negatively charged acenes if we assume that the overlap of the lowest unoccupied molecular orbitals (LUMO) between cyanodienes is not significantly different from that between two neighboring acenes. The structures of the monoanions of cyanodienes are optimized under $D_{2h}$ geometry, and the vibronic interaction effects in the monoanions of cyanodienes are discussed. The vibration effect on the charge-transfer problem is also discussed. The C−C and C−N stretching $A_g$ modes around 1000−1500 $cm^{-1}$ are the main modes converting the neutral structures to the monoanions in cyanodienes. This can be confirmed from the calculational results that the C−C and C−N stretching $A_g$ modes around 1000−1500 $cm^{-1}$ strongly couple to the LUMO in cyanodienes. The total electron−phonon coupling constants ($l_{LUMO}$) for the monoanions of cyanodienes are estimated to be larger than those for the monoanions of acenes. The orbital patterns difference between the LUMO localized on carbon atoms located at the edge part of the carbon framework in acenes and the delocalized LUMO in cyanodienes due to electronegativity perturbation is the main reason that the $l_{LUMO}$ values for polycyanodienes are much larger than those for polyacenes. The relationships between the electron transfer and the electron−phonon interactions are discussed. The plot of the reorganization energies against the $l_{LUMO}$ values is found to be nearly linear. In view of the results, the relationships between the normal and possible superconducting states are briefly discussed.

## Introduction

In synthetic chemistry and material science, the search for new organic metals and superconductors has attracted a great deal of attention since the discovery of high electrical conductivity in conjugated polymers such as polyacetylene.[1] In modern physics and chemistry, the effect of vibronic interactions[2] in molecules and crystals has been an important topic. The role of the vibronic interactions in the normal and superconducting states of conjugated polymers has been qualitatively discussed by one of the authors.[3] Since a hypothetical molecular superconductor based on an exciton mechanism has been proposed by Little,[4] the superconductivity of molecular systems have been extensively investigated and many bis(ethylenedithio)tetrathiafulvalene (BEDT-TTF)-type organic superconductors[5,6] have been yielded by advances in the design and synthesis of molecular systems. The alkali-doped $A_3C_{60}$ complexes[7] were found to exhibit superconducting transition temperatures ($T_c$) of more than 30 K[8] and 40 K under pressure.[9] In a Bardeen−Cooper−Schrieffer (BCS)-type[10] strong coupling scenario in superconductivity in alkali-doped fullerenes,[11] pure intramolecular Raman-active modes have been suggested to be important. Haddon discussed the rehybridization of the $\pi$ orbitals and the 2s atomic orbitals which may also be useful in order to understand the *high* $T_c$ superconductivity of the $A_3C_{60}$ complexes.[12] In the crystals of naphthalene ($C_{10}H_8$), anthracene ($C_{14}H_{10}$), tetracene ($C_{18}H_{12}$), and pentacene ($C_{22}H_{14}$),[13] the electron−phonon interactions were proposed to dominate the charge transport. From a theoretical point of view, the possible superconductivity of polyacene has been proposed.[14] It is very intriguing to investigate the possible superconductivity in various molecular crystals.

Stritzer and Buckel[15] found an isotope effect in $T_c$ shortly after the discovery of palladium hydrides.[16] The $T_c$ of Pd−D was higher than that of Pd−H,[17] and an even larger inverse isotope effect for Pd−T was measured by Schirber et al.,[18] contrary to the expectations from a simple BCS theory. Furthermore, an inverse isotope effect due to H−D substitution in organic superconductivity was observed by Saito et al.[19] We expect from the inverse isotope effect on deuterium substitution observed by Saito et al.[19] that such inverse isotope effects can be widely observed in molecular organic superconductors.

In previous work, we have analyzed the electron−phonon interactions in the monocations of acenes.[20] And recently, the electron−phonon interactions in the positively charged acene were well studied on the basis of an experimental study of ionization spectra using high-resolution gas-phase photoelectron spectroscopy by Brédas et al.[21] This experimental result shows that our predicted frequencies for the vibrational modes, which play an essential role in the electron−phonon interactions as well as the total electron−phonon coupling constants,[20] are in excellent agreement with those obtained from the experimental research.[21]

Substitution of carbon with boron and nitrogen have been carried out, producing totally substituted boron nitride nanotubes (BN-NTs).[22] The structure of these new boron−nitrogen-

* Author to whom correspondence should be addressed. E-mail: kato@cc.nias.ac.jp. Phone: +81-95-838-4363. Fax: +81-95-838-5101.

10.1021/jp0404753 CCC: $27.50 
Published on Web 11/23/2004

**CHART 1**

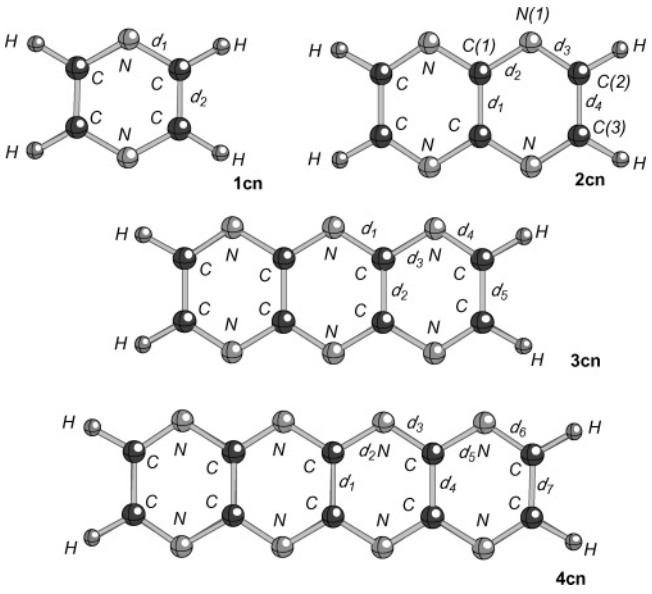


containing fullerenes and nanotubes have been studied and compared with that of carbon nanotubes (CNTs).[23−37] In the previous research, we compared the properties of the electron−phonon interactions in the monoanions of B,N-substituted acenes such as borazine $B_3N_3H_6$ (**1bn**), $B_5N_5H_8$ (**2bn**), and $B_7N_7H_{10}$ (**3bn**)[38] with those in the monoanions of acenes such as benzene $C_6H_6$ (**1a**), naphthalene $C_{10}H_8$ (**2a**), anthracene $C_{14}H_{10}$ (**3a**), and tetracene $C_{18}H_{12}$ (**4a**).[20] We found that the electron−phonon interactions in the monoanions in B,N-substituted acenes are as strong as those in the monoanions of acenes, but much lower frequency modes play a more essential role in the electron−phonon interactions in the monoanions of B,N-substituted acenes than in the monoanions of acenes and suggested that B,N-substitution in acenes is not effective way to seek possible higher-temperature superconductivity.

In this paper, we will discuss the electron−phonon interactions, intramolecular electron mobility, and the single charge transfer through molecule, estimate the reorganization energy for elementary charge transfer, and discuss the vibration effect onto the charge transfer problem, which is of interest for possible nanoelectronics applications, in the negatively charged polycyanodienes such as $C_4N_2H_4$ (**1cn**), $C_6N_4H_4$ (**2cn**), $C_8N_6H_4$ (**3cn**), and $C_{10}N_8H_4$ (**4cn**) (Chart 1). We compare the calculational results for the negatively charged polycyanodienes with those for the negatively charged acenes and B,N-substituted acenes to investigate how the properties of the electron−phonon interactions, intramolecular electron mobility, and the electron transfer are changed by electronegativity perturbation[39] in acenes. In cyanodienes, the edge CH part of acene is substituted by N atoms. We can expect that in the monoanions of cyanodienes the electron−phonon interactions become much stronger, and the high-frequency modes play an essential role in the electron−phonon interactions because the lowest unoccupied molecular orbitals (LUMO) are delocalized due to electronegativity perturbation on acenes.

## Theoretical Background

**Vibronic Coupling Constants.** We discuss a theoretical background for the orbital vibronic constants[2a] in **1cn**, **2cn**, **3cn**, and **4cn** with $D_{2h}$ geometry. Here, we take a one-electron approximation into account; the vibronic coupling constant of the vibrational modes to the electronic states in the monoanions of cyanodienes is defined as a sum of orbital vibronic coupling constants from all the occupied orbitals $i$[2a]

$$g_{\text{electronic state}} = \sum_{i}^{\text{occupied}} g_i. \tag{1}$$

Considering the one-electron approximation and that the first-order derivatives of the total energy vanish in the ground state at the equilibrium $D_{2h}$ structure in neutral **1cn**, **2cn**, **3cn**, and **4cn** ($g_{\text{neutral}} = \sum_i^{\text{HOMO}} g_i = 0$) and that one electron must be injected into the LUMO to generate the monoanions, the vibronic coupling constant of the vibronic active modes to the electronic states of the monoanions of cyanodienes can be defined by

$$g_{\text{monoanion}}(\omega_m) = g_{\text{LUMO}}(\omega_m) \tag{2}$$

The numbers of the vibronic active $A_g$ vibrational modes are 5, 7, 9, and 11, respectively. In such a case, we must consider multimode problems, but in the limit of linear vibronic coupling one can treat each set of modes (i.e., each mode index $m$) independently.[2]

Let us look into the vibronic coupling of the $A_g$ vibrational modes to the LUMO in cyanodienes. The dimensionless orbital vibronic coupling constant of the $m$th $A_g$ modes in cyanodienes is defined by

$$g_{\text{LUMO}}(\omega_m) = \frac{1}{\hbar\omega_m}\left\langle \text{LUMO}\left|\left|\left(\frac{\partial h_{Agm}}{\partial q_{Agm}}\right)_0\right|\right|\text{LUMO}\right\rangle \tag{3}$$

where $q_{A_{gm}}$ is the dimensionless normal coordinate[40] of the $m$th vibrational mode and $h_{A_{gm}}$ is the vibronic coupling matrix of the $m$th $A_g$ modes in cyanodienes.

**Electron−Phonon Coupling Constants.** In the previous section, the vibronic interactions in free cyanodienes were described. We set up an assumption to apply the calculated vibronic coupling constants to the solid-state properties of cyanodienes. We assume that the conduction band of the monoanion crystals of cyanodienes consists of the LUMOs because cyanodienes consist of strongly bonded molecules arranged on a lattice with weak van der Waals intermolecular bonds. Electron−phonon coupling constants of the $A_g$ modes in cyanodienes are defined as

$$l_{\text{LUMO}}(\omega_m) = g^2_{\text{LUMO}}(\omega_m)\hbar\omega_m \tag{4}$$

## Optimized Structures of Polycyanodienes

The structures of polycyanodienes were optimized under $D_{2h}$ symmetry, using the hybrid Hartree−Fock/density functional theory method of Becke,[41] and Lee, Yang, and Parr[42] (B3LYP) and the 6-31G* basis set.[43] The GAUSSIAN 98 program package[44] was used for our theoretical analyses. Optimized structures of these molecules are listed in Table 1. Furthermore, selected vibronic active modes and the frontier orbitals in polycyanodienes are shown in Figures 1 and 2, respectively. Each structure was confirmed to be a minimum on each energy surface. According to our calculations, the energy differences

**TABLE 1: C−C and C−N Distances in the Neutral Cyanodienes**

| | $d_1$ | $d_2$ | $d_3$ | $d_4$ | $d_5$ | $d_6$ | $d_7$ |
|---|---|---|---|---|---|---|---|
| **1cn** | 1.355 | 1.355 | | | | | |
| **2cn** | 1.430 | 1.361 | 1.316 | 1.424 | | | |
| **3cn** | 1.336 | 1.446 | 1.374 | 1.306 | 1.437 | | |
| **4cn** | 1.456 | 1.349 | 1.325 | 1.457 | 1.379 | 1.302 | 1.445 |

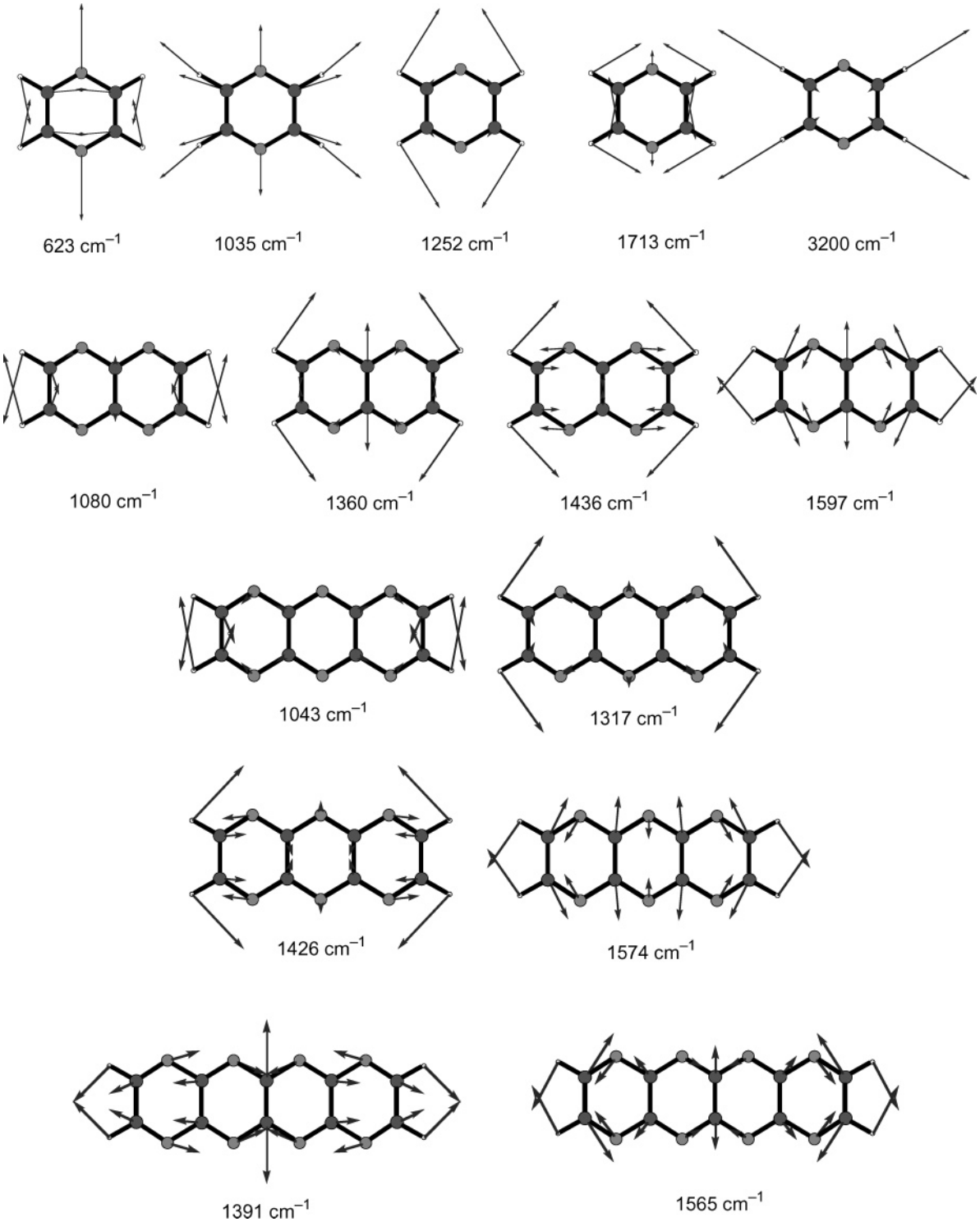


**Figure 1.** Selected vibronic active modes in cyanodienes.

between the HOMO and LUMO of **1cn**, **2cn**, **3cn**, and **4cn** are 5.16, 3.97, 3.19, and 2.68 eV, respectively, and those of **1a**, **2a**, **3a**, and **4a** are 6.80, 4.83, 3.59, and 2.78 eV, respectively. Therefore, the HOMO−LUMO gaps in cyanodienes are slightly smaller than those in acenes.

### Electron−Phonon Interactions in the Monoanions of Polycyanodienes

We carried out vibrational analyses of polycyanodienes at the B3LYP/6-31G* level of theory. We next calculated first-order derivatives at this equilibrium structure on each orbital energy surface by distorting the molecule along the $A_g$ modes of **1cn**, **2cn**, **3cn**, and **4cn** to obtain orbital vibronic coupling constants defined by eq 3.[2a,20,38] We can estimate the electron−phonon coupling constants from the dimensionless orbital vibronic coupling constants by using eq 4. The calculated electron−phonon coupling constants in the monoanions of **1cn**, **2cn**, **3cn**, and **4cn** are shown in Figure 3. Furthermore, the calculated reduced masses and the electron−phonon coupling constants for the monoanions of **1cn** and **2cn** are listed in Tables 2 and 3, respectively.

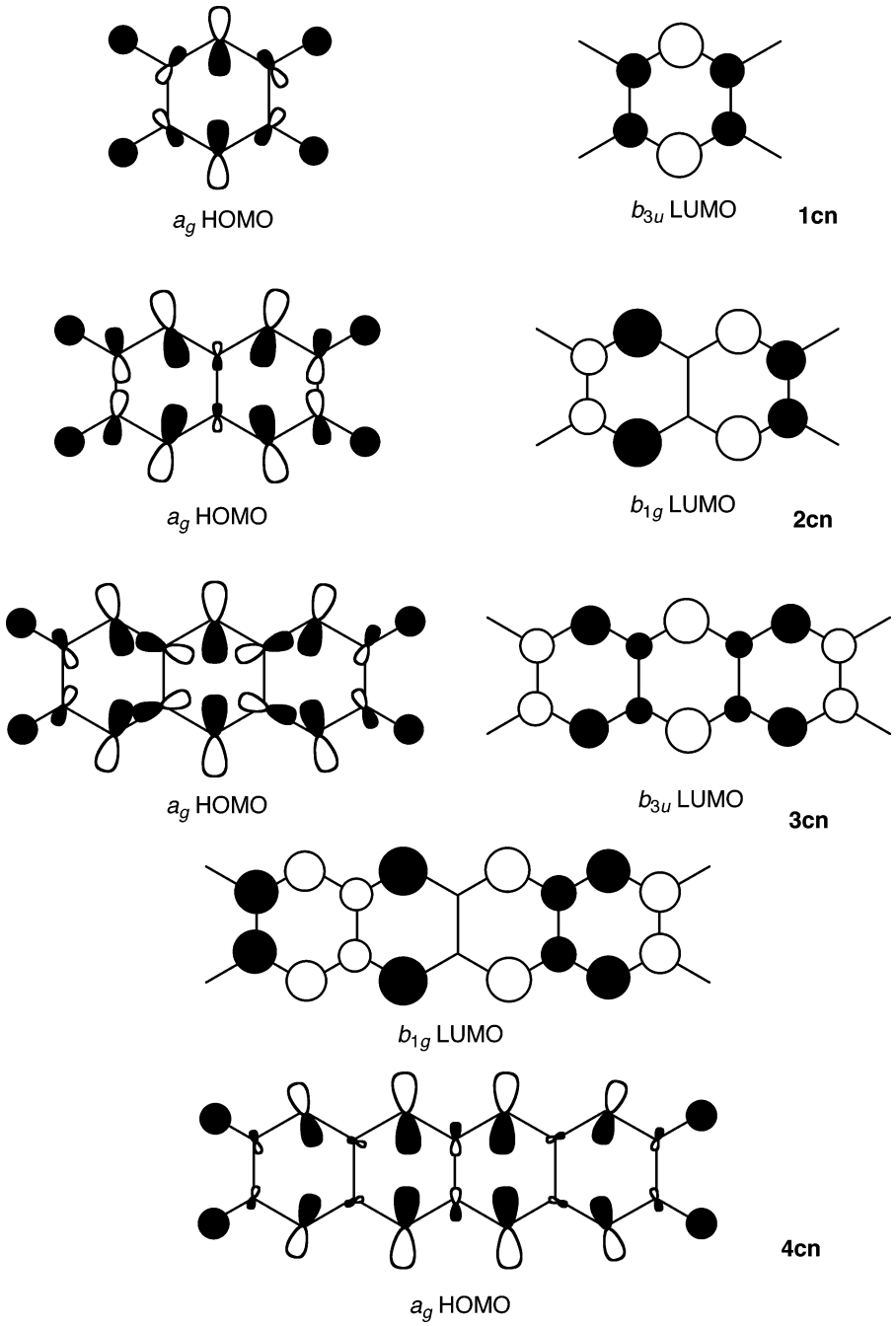


**Figure 2.** The phase patterns of the frontier orbitals in cyanodienes.

**TABLE 2: Calculated Reduced Masses and the Electron−Phonon Coupling Constants (eV) for the Monoanion of 1cn**

| | $A_g$ (623) | $A_g$ (1035) | $A_g$ (1252) | $A_g$ (1713) | $A_g$ (3200) | total |
|---|---|---|---|---|---|---|
| red. mass | 8.80 | 7.53 | 1.11 | 5.97 | 1.10 | |
| $l_{LUMO}(\omega_m)$ (eV) | 0.086 | 0.154 | 0.052 | 0.183 | 0.003 | 0.478 |

**TABLE 3: Calculated Reduced Masses and the Electron−Phonon Coupling Constants (eV) for the Monoanion of 2cn**

| | $A_g$ (555) | $A_g$ (775) | $A_g$ (1080) | $A_g$ (1360) | $A_g$ (1436) | $A_g$ (1597) | $A_g$ (3187) | total |
|---|---|---|---|---|---|---|---|---|
| red. mass | 8.99 | 9.83 | 2.33 | 2.92 | 3.08 | 6.52 | 1.10 | |
| $l_{LUMO}(\omega_m)$ (eV) | 0.002 | 0.022 | 0.033 | 0.053 | 0.098 | 0.130 | 0.000 | 0.338 |

Let us first look into the electron−phonon interactions between the $A_g$ modes and the $b_{3u}$ LUMO in **1cn**. We can see from this figure that the $A_g$ mode of 1713 $cm^{-1}$ can the most strongly couple to the $b_{3u}$ LUMO in **1cn**. When **1cn** is distorted along the $A_g$ mode of 1713 $cm^{-1}$ toward the same direction as shown in Figure 1, the bonding interactions between two neighboring carbon atoms in the $b_{3u}$ LUMO become stronger, and the antibonding interactions between two neighboring carbon and nitrogen atoms become weaker, and thus the $b_{3u}$ LUMO is significantly stabilized in energy. This is the reason the $A_g$ mode of 1713 $cm^{-1}$ can the most strongly couple to the $b_{3u}$ LUMO in **1cn**. The $A_g$ mode of 1035 $cm^{-1}$ also strongly couples to the $b_{3u}$ LUMO in **1cn**. When **1cn** is distorted along the $A_g$ mode of 1035 $cm^{-1}$, the antibonding interactions between two neighboring carbon and nitrogen atoms in the $b_{3u}$ LUMO become significantly weaker, and thus the $b_{3u}$ LUMO is significantly stabilized in energy by such a distortion. However, the bonding interactions between two neighboring carbon atoms

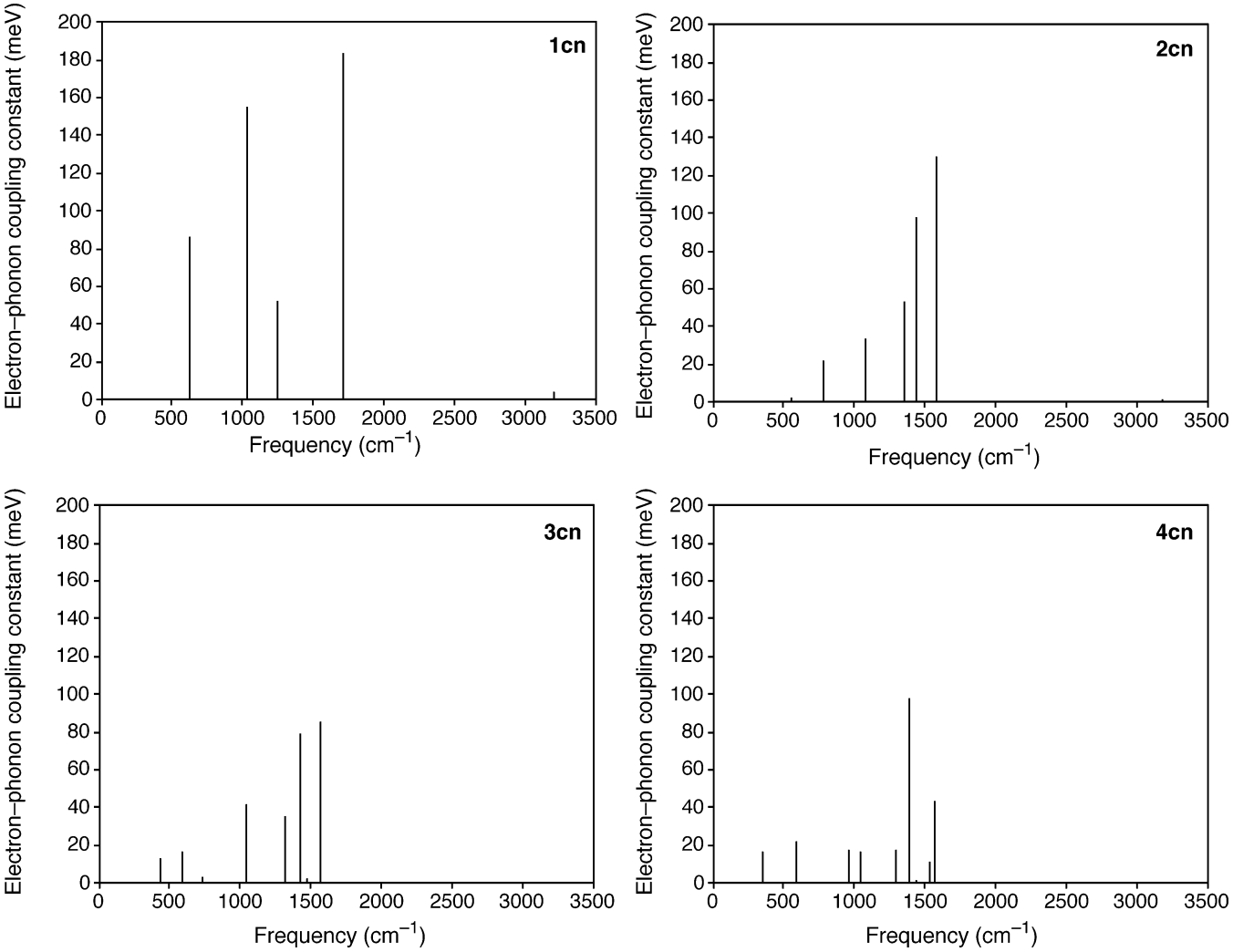


**Figure 3.** Electron−phonon coupling constants for the monoanions of polycyanodienes.

become also slightly weaker by such a distortion, and the $b_{3u}$ LUMO would be slightly destabilized in energy. Such stabilization and destabilization effects are compensated by each other. Therefore, the $A_g$ mode of 1035 $cm^{-1}$ affords a slightly smaller electron−phonon coupling constant than that of the $A_g$ mode of 1713 $cm^{-1}$ in the monoanion of **1cn**. Furthermore, the $A_g$ mode of 623 $cm^{-1}$ also somewhat strongly couples to the $b_{3u}$ LUMO in **1cn**. The reduced masses for the $A_g$ modes of 623, 1035, and 1713 $cm^{-1}$ are large and are 8.80, 7.53, and 5.97, respectively, in **1cn**. Therefore, the displacements of carbon and nitrogen are large in these modes. It is rational that the $A_g$ modes of 623, 1035, and 1713 $cm^{-1}$, in which the displacements of carbon and nitrogen atoms are larger, can strongly couple to the $b_{3u}$ LUMO localized on carbon and nitrogen atoms. However, the reduced masses for the $A_g$ modes of 1252 and 3200 $cm^{-1}$ are 1.11 and 1.10, respectively. It is rational that the $A_g$ modes of 1252 and 3200 $cm^{-1}$, in which the displacements of carbon and nitrogen atoms are small, cannot strongly couple to the $b_{3u}$ LUMO localized on carbon and nitrogen atoms. This is the reason that the $A_g$ modes of 623, 1035, and 1713 $cm^{-1}$ can more strongly couple to the $b_{3u}$ LUMO than the $A_g$ modes of 1252 and 3200 $cm^{-1}$ in **1cn**.

Let us look into the electron−phonon interactions between the $A_g$ modes and the $b_{1g}$ LUMO in **2cn**. We can see from Figure 3 that the $A_g$ mode of 1597 $cm^{-1}$ strongly couples to the $b_{1g}$ LUMO in **2cn**. This can be understood as follows. When **2cn** is distorted along the $A_g$ mode of 1597 $cm^{-1}$, the bonding interactions between two neighboring carbon atoms in the $b_{1g}$ LUMO become significantly weaker, and the antibonding interactions between two neighboring carbon and nitrogen atoms become significantly stronger, and thus the $b_{1g}$ LUMO is significantly destabilized in energy by such a distortion in **2cn**. This is the reason that the $A_g$ mode of 1597 $cm^{-1}$ can strongly couple to the $b_{1g}$ LUMO in **2cn**. The $A_g$ mode of 1436 $cm^{-1}$ can also strongly couple to the $b_{1g}$ LUMO in **2cn**. When **2cn** is distorted along the $A_g$ mode of 1436 $cm^{-1}$, the antibonding interactions between two neighboring carbon and nitrogen atoms in the $b_{1g}$ LUMO in **2cn** become stronger, and thus the $b_{1g}$ LUMO is significantly destabilized in energy by such a distortion in **2cn**. This is the reason that the $A_g$ mode of 1436 $cm^{-1}$ strongly couples to the $b_{1g}$ LUMO in **2cn**. Apart from the C−H stretching $A_g$ mode of 3187 $cm^{-1}$, the electron−phonon coupling constant increases with an increase in frequency in **2cn**. In the low frequency modes, which have similar characteristics to those of acoustic modes of phonons in solids, all atoms move toward the similar direction. Therefore, the orbital interactions between two neighboring atoms do not significantly change when **2cn** is distorted along the low frequency $A_g$ modes. This is the reason that the electron−phonon coupling decreases with a decrease in frequency in **2cn**. The C−H stretching mode of 3187 $cm^{-1}$ hardly couples to the $b_{1g}$ LUMO in **2cn**. The reduced mass for the $A_g$ mode of 3187 $cm^{-1}$ is 1.10, in which the displacements of carbon and nitrogen atoms are very small. The $b_{1g}$ LUMO is localized on carbon

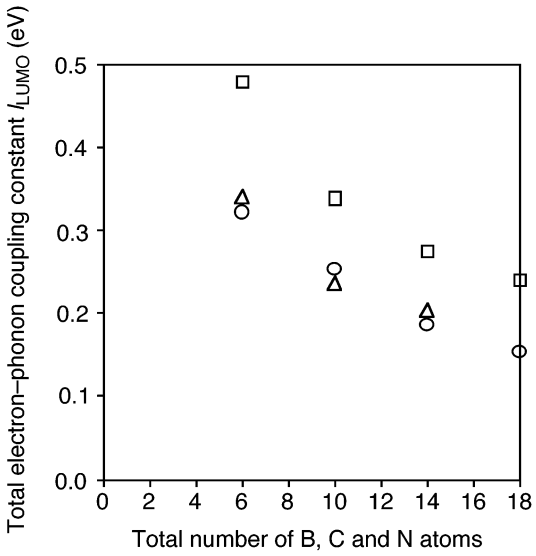


**Figure 4.** The total electron−phonon coupling constants as a function of the number of boron, carbon, and nitrogen atoms in the monoanions of acenes, B,N-substituted acenes, and cyanodienes. The circles, triangles, and squares represent the $l_{LUMO}$ values for acenes, B,N-substituted acenes, and cyanodienes, respectively.

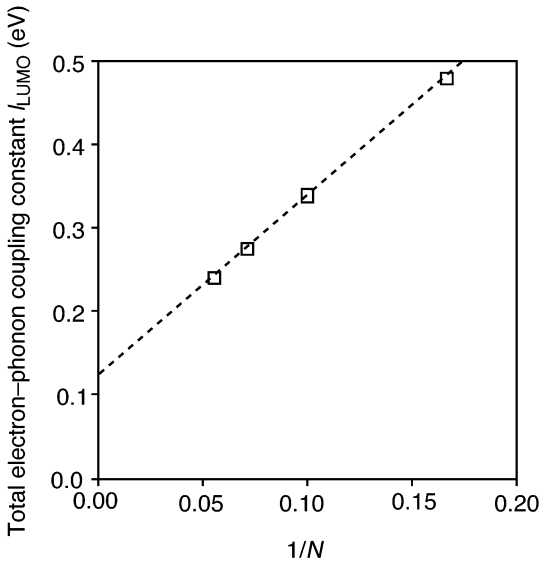


**Figure 5.** Total electron−phonon coupling constants as a function of $1/N$ in the monoanions of cyanodienes.

and nitrogen atoms in **2cn**. It is rational that the $A_g$ mode of 3187 $cm^{-1}$, in which the displacements of carbon and nitrogen atoms are very small, hardly couples to the $b_{1g}$ LUMO localized on carbon and nitrogen atoms in **2cn**. Similar discussions can be made in the monoanions of **3cn** and **4cn**; the C−C stretching modes around 1500 $cm^{-1}$ can strongly couple to the LUMO.

### Total Electron−Phonon Coupling Constants in Negatively Charged Cyanodienes

Let us next discuss the total electron−phonon coupling constants in the monoanions ($l_{LUMO}$) of cyanodienes and compare the calculational results for cyanodienes with those for acenes. The $l_{LUMO}$ values for cyanodienes are defined as

$$l_{LUMO} = \sum_m l_{LUMO}(\omega_m) = \sum_m g^2_{LUMO}(\omega_m)\hbar\omega_m \qquad (5)$$

The $l_{LUMO}$ values as a function of the number of carbon and nitrogen atoms in acenes, B,N-substituted acenes, and cyanodienes are shown in Figure 4.

The $l_{LUMO}$ values are estimated to be 0.478, 0.338, 0.275, and 0.240 eV for **1cn**, **2cn**, **3cn**, and **4cn**, respectively, whereas they are estimated to be 0.322, 0.255, 0.186, and 0.154 eV for **1a**, **2a**, **3a**, and **4a**, respectively, and they are estimated to be 0.340, 0.237, and 0.203 eV for **1bn**, **2bn**, and **3bn**, respectively. Therefore, the $l_{LUMO}$ values decrease with an increase in molecular size in acenes, B,N-substituted acenes, and cyanodienes.

The $l_{LUMO}$ values for cyanodienes are much larger than those for acenes. This can be understood in view of the orbital patterns of the LUMO in acenes and cyanodienes. The LUMOs of acenes are rather localized on carbon atoms located at the edge part of the carbon framework. Therefore, the nonbonding characteristic is significant in the LUMOs in acenes. However, the LUMO of cyanodienes is delocalized, and the electron density on carbon atoms as well as on nitrogen atoms located at the edge part of the CN framework is high in the LUMO in cyanodienes. Therefore, the orbital interactions between two neighboring atoms in the LUMO in cyanodienes are stronger than those in the LUMO in acenes. This is the reason that the $l_{LUMO}$ values for cyanodienes are much larger than those for acenes. Let us next discuss why the LUMOs of acenes are rather localized on carbon atoms located at the edge part of carbon framework, whereas those of cyanodienes are delocalized, and the electron density on carbon atoms as well as on nitrogen atoms is high in the LUMO in cyanodienes. In general, due to electronegativity perturbation,[39] the $\pi$ bonding orbitals are weighted more heavily on the atoms that are more electronegative, and the $\pi$ antibonding orbitals are weighted more heavily on the atoms that are less electronegative. As described above, the LUMOs are rather localized on carbon atoms that are located at the edge part of the carbon framework in acenes. In cyanodienes, carbon atoms with high electron density in the LUMO, located at the edge part of the carbon framework of acenes, are substituted by nitrogen atoms with the higher electronegativity. Therefore, the electron density on the nitrogen atoms in the LUMO in cyanodienes is lower than that of the carbon atoms located at the edge part of carbon framework in the LUMO of acenes, and the electron density on carbon atoms that are not located at the edge part of the CN framework in the LUMO in cyanodienes is higher than that on carbon atoms that are not located at the edge part of the carbon framework in the LUMO in acenes. This is the reason that the LUMOs of acenes are rather localized on carbon atoms located at the edge part of the carbon framework, whereas those of cyanodienes are delocalized, and the electron density on carbon atoms as well as on nitrogen atoms is high in cyanodienes.

### Polycyanodienes

Let us next estimate the $l_{LUMO}$ values for polycyanodienes with $D_{2h}$ geometry. The $l_{LUMO}$ values for polycyanodienes with $D_{2h}$ geometry as a function of $1/N$ values are shown in Figure 5, where $N$ is the number of carbon and nitrogen atoms in polycyanodienes. We can see from this figure that the $l_{LUMO}$ values for cyanodienes with $D_{2h}$ geometry are approximately inversely proportional to the number of carbon and nitrogen atoms in each series, as suggested in previous research.[21] From this figure, the $l_{LUMO}$ value for polycyanodiene ($N \rightarrow \infty$) is estimated to be 0.122 eV. The $l_{LUMO}$ value for polyacene with $D_{2h}$ geometry was estimated to be 0.019 eV.

The $l_{LUMO}$ values for polycyanodienes are estimated to be much larger than those for polyacenes. Therefore, the orbital

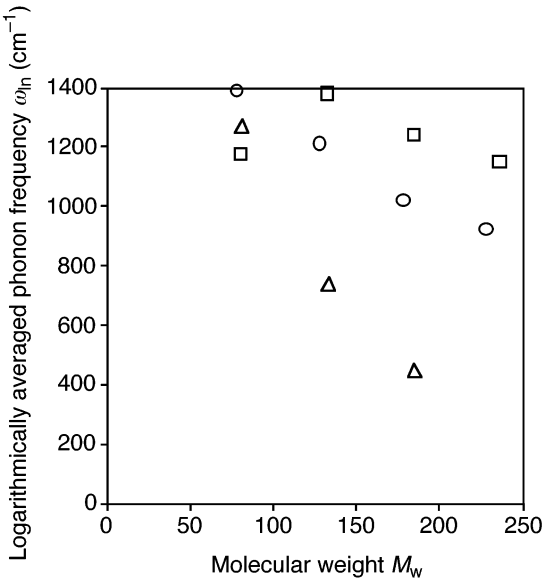


**Figure 6.** The logarithmically averaged phonon frequencies as a function of molecular weight. The circles, triangles, and squares represent the $\omega_{ln}$ values for acenes, B,N-substituted acenes, and cyanodienes, respectively.

patterns difference between the LUMO localized on carbon atoms located at the edge part of the carbon framework in acenes and the delocalized LUMO in cyanodienes due to electronegativity perturbation is the main reason that the $l_{LUMO}$ values for polycyanodienes are much larger than those for polyacenes with $D_{2h}$ geometry.

### The Logarithmically Averaged Phonon Frequencies

Let us next look into the logarithmically averaged phonon frequencies $\omega_{ln}$ for the monoanions of cyanodienes, denoting the frequencies of the vibrational modes which play an essential role in the electron−phonon interactions. The $\omega_{ln}$ values for the monoanions of cyanodienes are defined as

$$\omega_{ln} = \exp\left\{\sum_m \frac{l_{LUMO}(\omega_m)\ln\omega_m}{l_{LUMO}}\right\} \quad (6)$$

The $\omega_{ln}$ values as a function of molecular weight $M_w$ in the monoanions of acenes, B,N-substituted acenes, and cyanodienes are shown in Figure 6. The $\omega_{ln}$ values are estimated to be 1179, 1381, 1242, and 1150 cm$^{-1}$ for the monoanions of **1cn**, **2cn**, **3cn**, and **4cn**, respectively, and 1390, 1212, 1023, and 926 cm$^{-1}$ for the monoanions of **1a**, **2a**, **3a**, and **4a**, respectively. Therefore, apart from **1cn**, the $\omega_{ln}$ values for the monoanions of acenes and cyanodienes decrease with an increase in molecular weights. This is in qualitative agreement with a tendency; light mass will lead to higher values of $\omega_{ln}$. But it should be noted that the $\omega_{ln}$ values for the monoanions of cyanodienes with $D_{2h}$ geometry are larger than those for the monoanions of acenes with $D_{2h}$ geometry. As described above, the LUMO of acenes is rather localized on carbon atoms located at the edge part of the carbon framework in acenes, and thus the nonbonding characteristics are significant. Therefore, the orbital interactions between two neighboring carbon atoms are weak. However, due to electronegativity perturbation, the LUMO of cyanodienes is delocalized, and the electron density on carbon atoms as well as on nitrogen atoms located at the edge part of the CN framework is high, and thus the orbital interactions between two neighboring carbon and nitrogen atoms and between two neighboring carbon atoms in the LUMO are strong. This is the reason that the C−N and C−C stretching modes around 1500 cm$^{-1}$ in the monoanions of cyanodienes afford larger electron−phonon coupling constants than the C−C stretching modes around 1500 cm$^{-1}$ in the monoanions of acenes and the reason that the $\omega_{ln}$ values for the monoanions of cyanodienes are larger than those for the monoanions of acenes. Therefore, the orbital patterns difference between the delocalized LUMO in cyanodienes and the LUMO localized on carbon atoms located at the edge part of the carbon framework in acenes is the main reason that the $l_{LUMO}$ and $\omega_{ln}$ for the monoanions of cyanodienes are larger than those for the monoanions of acenes.

### The Effect of Electronegativity Perturbation on Electron−Phonon Interactions

Let us next discuss how the electronegativity perturbation is related to the characteristics of the electron−phonon interactions in negatively charged acenes. In this section, we compare the calculated results for the monoanions of cyanodienes with those for the monoanions of acenes and B,N-substituted acenes. The Pauling's electronegativity for boron, carbon, and nitrogen atoms are 2.55, 3.04, and 3.44, respectively.[45] These differences in electronegativity would account for the significant characteristics differences in the electron−phonon interactions between acenes, B,N-substituted acenes, and cyanodienes. The $l_{LUMO}$ values for B,N-substituted acenes are similar to those for acenes. However, the $\omega_{ln}$ values for the monoanions of **1bn**, **2bn**, and **3bn** were estimated to be 1273, 737, and 449 cm$^{-1}$, respectively. Therefore, the $\omega_{ln}$ values for the monoanions of B,N-substituted acenes decrease with an increase in molecular size much more rapidly than those for the monoanions of acenes. Therefore, the monoanions of acenes would exhibit higher temperature superconductivity than the monoanions of B,N-substituted acenes if we assume that the negatively charged nanosized molecular systems would exhibit superconductivity mainly caused by the vibronic interactions between the intramolecular vibrations and the LUMO. Both the $l_{LUMO}$ and $\omega_{ln}$ values for the monoanions of cyanodienes are larger than those for the monoanions of acenes. Therefore, the possible $T_c$ values for the monoanions of cyanodienes are estimated to be larger than those for the monoanions of acenes if the physical values originating from the intermolecular interactions (for example, density of states at the Fermi level) are not significantly different between these anions.

### Intramolecular Electron Mobility in Cyanodienes

Here, let us consider one-electron transfer assisted by molecular vibrations as a molecular model of the interaction of conduction electrons with vibration.[3,46] From analogy with the definition of the intrinsic intramolecular conductivity $\sigma_{intra,monoanion}$ for the monoanions of acenes and B,N-substituted acenes as discussed in previous research,[38] according to the definition suggested by Kivelson and Heeger,[3,46] we define that for the monoanions of cyanodienes $C_{N/2+1}N_{N/2-1}H_4$ as

$$\sigma_{intra,monoanion} \propto \frac{\omega_{ln,LUMO}\{(N/2+1)M_C + (N/2-1)M_N\}}{{l_{LUMO}}^2} \quad (7)$$

where $M_C$ and $M_N$ denote the masses of carbon and nitrogen atoms, respectively. The calculated $\sigma_{intra,monoanion}$ values as a function of $N$ are shown in Figure 7. We can see from Figure 7 that the $\sigma_{intra,monoanion}$ value slightly increases with an increase

**TABLE 4: C−C and C−N Distances in the Monoanions of Cyanodienes[a]**

| | $d_1$ | $d_2$ | $d_3$ | $d_4$ | $d_5$ | $d_6$ | $d_7$ |
|---|---|---|---|---|---|---|---|
| **1cn**$^-$ | 1.383 | 1.374 | | | | | |
| | (+0.028) | (+0.019) | | | | | |
| **2cn**$^-$ | 1.464 | 1.357 | 1.351 | 1.384 | | | |
| | (+0.034) | (−0.004) | (+0.035) | (−0.040) | | | |
| **3cn**$^-$ | 1.348 | 1.460 | 1.359 | 1.335 | 1.399 | | |
| | (+0.012) | (+0.014) | (−0.015) | (+0.029) | (−0.038) | | |
| **4cn**$^-$ | 1.474 | 1.346 | 1.343 | 1.455 | 1.363 | 1.325 | 1.410 |
| | (+0.018) | (−0.003) | (+0.018) | (−0.002) | (−0.016) | (+0.023) | (−0.035) |

[a] The values in parentheses indicate the change of the C−C and C−N distances by electron doping in cyanodienes.

**TABLE 5: Estimated Ionization Energy, Electron Affinity, Hopping Barrier, and Reorganization Energy between Neutral Molecules and the Monoanions in Acenes and Cyanodienes**

| | ionization energy (eV) | electron affinity (eV) | hopping barrier (eV) | reorganization energy (eV) |
|---|---|---|---|---|
| **(1h)(1h**$^-$**) → (1h**$^-$**)(1h)** | 0.201 | −0.195 | 0.396 | 0.099 |
| **(1cn)(1cn**$^-$**) → (1cn**$^-$**)(1cn)** | 0.016 | −0.423 | 0.439 | 0.110 |
| **(2h)(2h**$^-$**) → (2h**$^-$**)(2h)** | 0.127 | −0.130 | 0.257 | 0.064 |
| **(2cn)(2cn**$^-$**) → (2cn**$^-$**)(2cn)** | 0.165 | −0.171 | 0.336 | 0.084 |
| **(3h)(3h**$^-$**) → (3h**$^-$**)(3h)** | 0.096 | −0.099 | 0.195 | 0.049 |
| **(3cn)(3cn**$^-$**) → (3cn**$^-$**)(3cn)** | 0.132 | −0.136 | 0.268 | 0.067 |
| **(4h)(4h**$^-$**) → (4h**$^-$**)(4h)** | 0.076 | −0.079 | 0.155 | 0.039 |
| **(4cn)(4cn**$^-$**) → (4cn**$^-$**)(4cn)** | 0.113 | −0.117 | 0.230 | 0.058 |

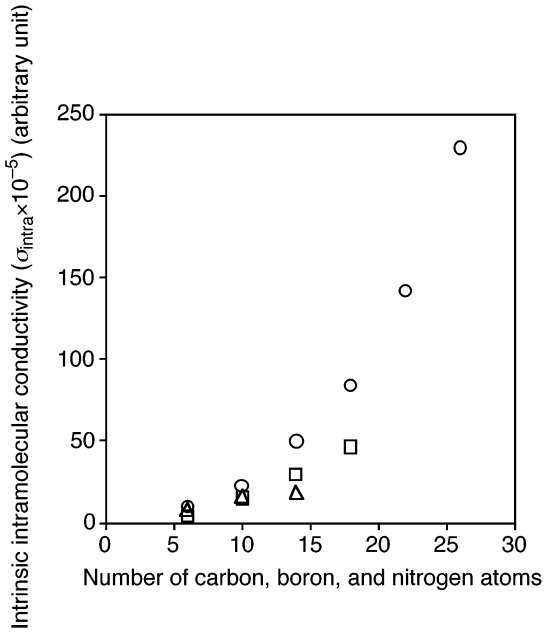


**Figure 7.** Intrinsic intramolecular conductivity as a function of the number of carbon, boron, and nitrogen atoms in the negatively charged acenes, B,N-substituted acenes, and cyanodienes. The circles, triangles, and squares represent the values for acenes, B,N-substituted acenes, and cyanodienes, respectively.

in molecular size from **1cn** ($\sigma_{intra,monoanion} = 3.9 \times 10^5$) to **4cn** ($\sigma_{intra,monoanion} = 46.3 \times 10^5$). This is because the $N$ and $l^2_{LUMO}$ values significantly increase and decrease, respectively, with an increase in molecular size in cyanodienes, whereas the $\omega_{ln,LUMO}$ values do not significantly change with an increase in molecular size in cyanodienes. The $\sigma_{intra,monoanion}$ values also increase with an increase in molecular size from **1a** ($\sigma_{intra,monoanion} = 9.7 \times 10^5$) to **4a** ($\sigma_{intra,monoanion} = 84.3 \times 10^5$). It should be noted that the $\sigma_{intra,monoanion}$ values for acenes are larger than those for cyanodienes. This is because the $l_{LUMO}$ values for cyanodienes are much larger than those for acenes even though the $\omega_{ln,LUMO}$ values for acenes are slightly smaller than those for cyanodienes. The main difference between acenes and cyanodienes is the difference of the $l_{LUMO}$ values rather than the $\omega_{ln,LUMO}$ values between these molecules. Such different strengths of the electron−phonon interactions come from electronegativity perturbation on acenes.

## Vibration Effects and Electron Transfer in Negatively Charged Cyanodienes

**Electron Transfer in the Negatively Charged Cyanodienes.** Let us next discuss the single charge transfer through the molecule under consideration, which is of interest for possible nanoelectronics applications. Here, we will estimate the reorganization energy for elementary charge transfer and will discuss the vibration effect onto the charge-transfer problem. We optimized the structures of these monoanions of cyanodienes. The optimized parameters of these monoanions are listed in Table 4. The estimated ionization energy, electron affinity, hopping barrier, and reorganization energy between neutral molecules and the monoanions in cyanodienes are listed in Table 5.

For example, we consider the Marcus-type electron-transfer diagram for **(1cn)(1cn**$^-$**) → (1cn**$^-$**)(1cn)**. That is, after the **1cn**$^-$ loses the electron, **1cn** relaxes toward the optimized geometry of neutral molecule. Simultaneously, the **1cn** upon accepting the electron distorts to the optimized geometry of the monoanion. Denoting the adiabatic ionization energy as $I_0$, the vertical (fixed geometry) ionization from the ground state of the monoanion of **1cn** costs an energy of $I_0 + 0.016$ eV (the energy difference between the neutral molecule and the monoanion *at the optimized geometry of the neutral molecule*), whereas the electron affinity of the monoanion of **1cn** (at its optimum geometry) is $I_0 - 0.423$ eV (the energy difference between the neutral molecule and the monoanion *at the optimized geometry of the monoanion*). Thus, isolated neutral **1cn** and the monoanion of **1cn** molecules with their optimized structures lead to a hopping barrier of 0.439 eV (ignoring polarization of the environment which might increase the barrier). Considering the Marcus-type electron transfer diagram, a net barrier can be estimated to be ∼0.439/4 = 0.110 eV. In a similar way, the reorganization energies between the neutral molecules and the corresponding monoanions are estimated to be 0.084, 0.067, and 0.058 eV for **2cn**, **3cn**, and **4cn**, respectively, and 0.099,

0.064, 0.049, and 0.039 eV for **1a**, **2a**, **3a**, and **4a**, respectively. It should be noted that the electronic interactions (orbital overlap) and steric interactions are ignored when we estimate the reorganization energies between the neutral molecules and the monoanions. For a good conductor with rapid electron transfer, the overlap of the LUMOs of these molecules should be sufficiently large. This requires interaction energies greater than the reorganization energies between the neutral molecules and the corresponding monoanions.

The reorganization energies between the neutral molecule and the corresponding monoanion for cyanodienes are larger than those for acenes. This means that the negatively charged cyanodienes would not be better conductors with slow electron transfer than the negatively charged acenes.

The reorganization energies decrease with an increase in molecular size in cyanodienes as well as in acenes. This means that the larger the molecular size of cyanodienes is, then the better conductor with rapid electron transfer this negatively charged molecule is, if we assume that the overlap of the LUMOs between two neighboring cyanodiene molecules do not significantly depend on the molecular size. However, the estimated $T_c$ values decrease with an increase in molecular size in the negatively charged acenes and cyanodienes.[20] There is an interesting paradox in conventional superconductivity; the higher resistivity at room temperature, the more likely it is that a metal will be a superconductor when cooled.[47] Therefore, the calculational results for the reorganization energies and the $T_c$ values in the negatively charged acenes are in qualitative agreement with such an interesting paradox, if these anions could exhibit superconductivity caused by the intramolecular vibronic interactions.

**Vibration Effects and the Optimized Structures of the Negatively Charged Cyanodienes.** Let us next look into the optimized structures of the monoanions of cyanodienes. We can see from Table 4 that the $d_3$ and $d_4$ values in the monoanion of **2cn** are much larger and smaller, respectively, than those in neutral **2cn**. This can be understood as follows. To generate the monoanion of **2cn**, one electron must be injected into the LUMO in **2cn**, in which the atomic orbitals between two neighboring N(1) and C(2) atoms and between two neighboring C(2) and C(3) atoms are combined out of phase and in phase, respectively, and thus form antibonding and bonding interactions, respectively. This is the reason that the $d_3$ and $d_4$ values become larger and smaller, respectively, by electron doping in the neutral **2cn**. However, the C−H bond lengths hardly change by electron doping in **2cn**. This is because the atomic orbitals between two neighboring carbon and hydrogen atoms form nonbonding interactions in the LUMO in **2cn**. Similar discussions can be made in **3cn** and **4cn**; the distances between two neighboring atoms, whose atomic orbitals are combined in phase (out of phase) in the LUMO, become smaller (larger) by electron doping.

Let us next look into the vibration effect onto the charge-transfer problem. We can see from Figure 1 and Table 4 that the $A_g$ mode of 1035 $cm^{-1}$ is the main mode converting the neutral **1cn** to the monoanion of **1cn**. This can be also confirmed from our calculational results that the $A_g$ modes of 1035 and 1713 $cm^{-1}$ very strongly couple to the LUMO in **1cn**. Furthermore, the $A_g$ modes of 1360, 1043, and 1391 $cm^{-1}$ are the main modes converting the neutral structures to the monoanions of **2cn**, **3cn**, and **4cn**, respectively. This can be also confirmed from our calculated results that these $A_g$ modes strongly couple to the LUMO.

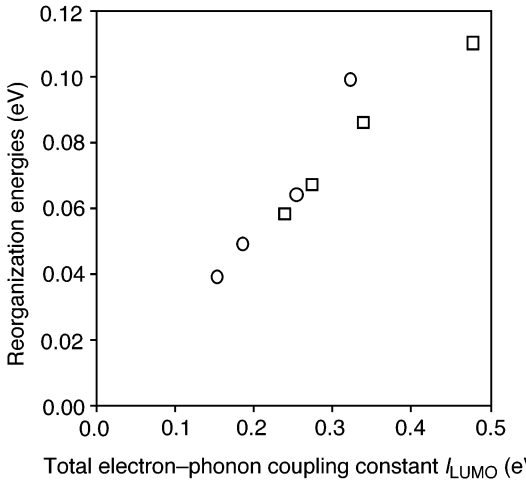


**Figure 8.** The relationships between reorganization energies and the total electron−phonon coupling constants. The circles and squares represent the values for acenes and cyanodienes, respectively.

### Relationships between the Electron Transfer and the Electron−Phonon Interactions

In Figure 8, the reorganization energies as a function of the total electron−phonon coupling constants are shown. In view of Figure 8, a plot of the reorganization energies against the total electron−phonon coupling constants is found to be nearly linear.

The reorganization energies decrease with an increase in molecular size in cyanodienes, as in acenes. This means that the larger the molecular size of cyanodienes is, then the better conductor with rapid electron transfer this negatively charged molecule is, if we assume that the overlaps of the LUMOs between two neighboring cyanodienes do not significantly depend on the molecular size. However, the estimated $l_{LUMO}$ value decreases with an increase in molecular size in cyanodienes. Therefore, in view of the linear relationships between the reorganization energies and the total electron−phonon coupling constants in the negatively charged cyanodienes, it is rational that our calculated results are in qualitatively agreement with an interesting paradox[47] as described above.

### Concluding Remarks

We discussed the single charge transfer through cyanodienes. The reorganization energies between the neutral molecules and the corresponding monoanions are estimated to be 0.110, 0.084, 0.067, and 0.058 eV for **1cn**, **2cn**, **3cn**, and **4cn**, respectively, and 0.099, 0.064, 0.049, and 0.039 eV for **1a**, **2a**, **3a**, and **4a**, respectively. Therefore, the reorganization energies between the neutral molecule and the corresponding monoanion for cyanodienes are larger than those for acenes. This means that the negatively charged cyanodienes would not be a better conductor with slow electron transfer than the negatively charged acenes.

We optimized the structures of the monoanions of cyanodienes under $D_{2h}$ geometry, and we discussed the vibronic interaction effects in the monoanions of cyanodienes. The bond distances between two neighboring carbon and nitrogen atoms and between two neighboring carbon atoms, whose atomic orbitals are combined in phase (out of phase) in the LUMO, become shorter (longer) by electron doping.

We also discussed the vibration effect on the charge-transfer problem. The $A_g$ modes of 1035, 1360, 1043, and 1391 $cm^{-1}$ are the main modes converting the neutral structures to the monoanions in **1cn**, **2cn**, **3cn**, and **4cn**, respectively. These

results can also be confirmed from our calculated results that these $A_g$ modes very strongly couple to the LUMO in cyanodienes.

We estimated the electron−phonon coupling constants in the monoanions of cyanodienes. The C−C and C−N stretching $A_g$ modes around 1000−1600 $cm^{-1}$ afford large electron−phonon coupling constants in the monoanions of cyanodienes. The $l_{LUMO}$ values are estimated to be 0.478, 0.338, 0.275, and 0.240 eV for **1cn**, **2cn**, **3cn**, and **4cn**, respectively, whereas they were estimated to be 0.322, 0.255, 0.186, and 0.154 eV for **1a**, **2a**, **3a**, and **4a**, respectively. Therefore, the $l_{LUMO}$ values decrease with an increase in molecular size in both acenes and cyanodienes. The $l_{LUMO}$ values for cyanodienes are much larger than those for acenes. This can be understood as follows. The LUMOs of acenes are rather localized on carbon atoms located at the edge part of the carbon framework. Therefore, the nonbonding characteristic is significant in the LUMOs in acenes. However, the LUMO of cyanodienes is delocalized and in which the electron density on carbon atoms as well as on nitrogen atoms located at the edge part of the CN framework is high in cyanodienes. Therefore, the orbital interactions between two neighboring atoms in the LUMO in cyanodienes are stronger than those in the LUMO in acenes, because of the electronegativity perturbation on acenes. This is the reason that the $l_{LUMO}$ values for cyanodienes are much larger than those for acenes. We also estimated the $l_{LUMO}$ value for polycyanodienes with $D_{2h}$ geometry by considering that the $l_{LUMO}$ values are approximately inversely proportional to the molecular size. The $l_{LUMO}$ value for polycyanodienes (0.122 eV) is estimated to be larger than those for polyacenes (0.019 eV) with $D_{2h}$ geometry. The orbital patterns difference between the LUMO localized on carbon atoms at the edge part of the carbon framework in acenes and the delocalized LUMO in cyanodienes due to electronegativity perturbation is the main reason that the $l_{LUMO}$ values for polycyanodienes are much larger than those for polyacenes with $D_{2h}$ geometry. The $\omega_{ln}$ values for the monoanions of cyanodienes are similar to those for the monoanions of acenes and are much larger than those for the monoanions of B,N-substituted acenes.

We investigated the relationships between the total electron−phonon coupling constants and the reorganization energies in the negatively charged cyanodienes. The plot of the reorganization energies against the total electron−phonon coupling constants is found to be nearly linear. The reorganization energies between the neutral molecules and corresponding monoanions decrease with an increase in molecular size in cyanodienes. This means that the larger the molecular size of acenes and cyanodienes are, then the better conductor with rapid electron transfer these negatively charged molecules are, if we assume that the overlap of the LUMOs between two neighboring molecules do not significantly depend on the molecular size. However, the $l_{LUMO}$ value decreases with an increase in molecular size in acenes and cyanodienes. Therefore, in view of the relationships, it is rational that our calculated results are in qualitative agreement with an interesting paradox in conventional superconductivity; the higher resistivity at room temperature, the more likely it is that a metal will be a superconductor when cooled, if these monoanions could exhibit superconductivity mainly caused by the intramolecular vibronic interactions.

**Acknowledgment.** We performed this study under the Project of Academic Frontier Center at Nagasaki Institute of Applied Science. This work is partly supported by a Grant-in-Aid for Scientific Research from the Japan Society for the Promotion of Science (JSPS-15350114, JSPS-16560618).

## References and Notes

(1) (a) Shirakawa, H.; Louis, E. J.; MacDiarmid, A. G.; Chiang, C. K.; Heeger, A. J. *J. Chem. Soc., Chem. Commun.* **1977**, *1977*, 578. (b) Chiang, C. K.; Park, Y. W.; Heeger, A. J.; Shirakawa, H.; Louis, E. J.; MacDiarmid, A. G. *Phys. Rev. Lett.* **1977**, *39*, 1098. (c) Chiang, C. K.; Druy, M. A.; Gau, S. C.; Heeger, A. J.; Louis, E. J.; MacDiarmid, A. G.; Park, Y. W.; Shirakawa, H. *J. Am. Chem. Soc.* **1978**, *100*, 1013.

(2) (a) Bersuker, I. B. *The Jahn−Teller Effect and Vibronic Interactions in Modern Chemistry*; Plenum: New York, 1984. (b) Bersuker, I. B.; Polinger, V. Z. *Vibronic Interactions in Molecules and Crystals*; Springer: Berlin, 1989.

(3) Yamabe, T. *Conjugated Polymers and Related Materials*; Oxford University Press: Oxford, 1993; p 443.

(4) Little, W. A. *Phys. Rev.* **1964**, *A134*, 1416.

(5) (a) Jérome, D.; Mazaud, A.; Ribault, M.; Bechgaad, K. *J. Phys. Lett.* (France) **1980**, *41*, L95. (b) Ribault, M.; Benedek, G.; Jérome, D.; Bechgaad, K. *J. Phys. Lett.* (France) **1980**, *41*, L397.

(6) Reviews and books: (a) Jérome, D.; Schulz, H. J. *Adv. Phys.* **1982**, *31*, 299. (b) Ishiguro, T.; Yamaji, K. *Organic Superconductors*; Springer: Berlin, 1990. (c) Williams, J. M.; Ferraro, J. R.; Thorn, R. J.; Karlson, K. D.; Geiser, U.; Wang, H. H.; Kini, A. M.; Whangbo, M.-H. *Organic Superconductors*; Prentice Hall: Englewood Cliffs, NJ, 1992.

(7) (a) Hebard, A. F.; Rosseinsky, M. J.; Haddon, R. C.; Murphy, D. W.; Glarum, S. H.; Palstra, T. T. M.; Ramirez, A. P.; Kortan, A. R. *Nature* **1991**, *350*, 600. (b) Rosseinsky, M. J.; Ramirez, A. P.; Glarum, S. H.; Murphy, D. W.; Haddon, R. C.; Hebard, A. F.; Palstra, T. T. M.; Kortan, A. R.; Zahurak, S. M.; Makhija, A. V. *Phys. Rev. Lett.* **1991**, *66*, 2830.

(8) Tanigaki, K.; Ebbesen, T. W.; Saito, S.; Mizuki, J.; Tsai, J. S.; Kubo, Y.; Kuroshima, S. *Nature* **1991**, *352*, 222.

(9) Palstra, T. T. M.; Zhou, O.; Iwasa, Y.; Sulewski, P. E.; Fleming, R. M.; Zegarski, B. R. *Solid State Commun.* **1995**, *93*, 327.

(10) (a) Schrieffer, J. R. *Theory of Superconductivity*; Addison-Wesley: Reading, MA, 1964. (b) de Gennes, P. G. *Superconductivity of Metals and Alloys*; Benjamin: New York, 1966.

(11) (a) Varma, C. M.; Zaanen, J.; Raghavachari, K. *Science* **1991**, *254*, 989. (b) Lannoo, M.; Baraff, G. A.; Schlüter, M.; Tomanek, D. *Phys. Rev. B: Condens. Matter Mater. Phys.* **1991**, *44*, 12106. (c) Asai, Y.; Kawaguchi, Y. *Phys. Rev. B: Condens. Matter Mater. Phys.* **1992**, *46*, 1265. (d) Faulhaber, J. C. R.; Ko, D. Y. K.; Briddon, P. R. *Phys. Rev. B: Condens. Matter Mater. Phys.* **1993**, *48*, 661. (e) Antropov, V. P.; Gunnarsson, O.; Lichtenstein, A. I.; *Phys. Rev. B: Condens. Matter Mater. Phys.* **1993**, *48*, 7651. (f) Gunnarsson, O. *Phys. Rev. B: Condens. Matter Mater. Phys.* **1995**, *51*, 3493. (g) Gunnarsson, O.; Handschuh, H.; Bechthold, P. S.; Kessler, B.; Ganteför, G.; Eberhardt, W. *Phys. Rev. Lett.* **1995**, *74*, 1875. (h) Dunn, J. L.; Bates, C. A. *Phys. Rev. B: Condens. Matter Mater. Phys.* **1995**, *52*, 5996. (i) Gunnarsson, O. *Rev. Mod. Phys.* **1997**, *69*, 575. (j) Devos, A.; Lannoo, M. *Phys. Rev. B: Condens. Matter Mater. Phys.* **1998**, *58*, 8236. (k) Gunnarsson, O. *Nature* **2000**, *408*, 528.

(12) Haddon, R. C. *Acc. Chem. Res.* **1992**, *25*, 127.

(13) (a) Silinch, E. A.; Capek, V. *Organic Molecular Crystals*; AIP: New York, 1994. (b) Warta, W.; Karl, N. *Phys. Rev. B: Condens. Matter Mater. Phys.* **1985**, *32*, 1172. (c) Warta, W.; Stehle, R.; Karl, N. *Appl. Phys. A: Mater. Sci. Process.* **1985**, *36*, 163.

(14) (a) Kivelson, S.; Chapman, O. L. *Phys. Rev. B: Condens. Matter Mater. Phys.* **1983**, *28*, 7236. (b) Mishima, A.; Kimura, M. *Synth. Met.* **1985**, *11*, 75.

(15) Stritzker, B.; Buckel, W. *Z. Physik* **1972**, *257*, 1.

(16) Skoskiewicz, T. *Phys. Status Solidi* 1972, *A11*, K123.

(17) Li, W.-H.; Lynn, J. W.; Stanley, H. B.; Udovic, T. J.; Shelton, R. N.; Klavins, P. *Phys. Rev. B: Condens. Matter Mater. Phys.* **1989**, *257*, 4119.

(18) Schirber, J. E.; Mintz, J. M.; Wall, W. *Solid State Commun.* **1984**, *52*, 837.

(19) Oshima, K.; Urayama, H.; Yamochi, H.; Saito, G. *J. Phys. Soc. Jpn. 57*, **1988**, 730.

(20) Kato, T.; Yamabe, T. *J. Chem. Phys.* **2001**, *115*, 8592.

(21) Coropceanu, V.; Filho, D. A. da Silva; Gruhn, N. E.; Bill, T. G.; Brédas, J. L. *Phys. Rev. Lett.* **2002**, *89*, 275503.

(22) Hamilton, E. J. M.; Dolan, S. E.; Mann, C. M., Colijn, H. O.; McDonald, C. A.; Shore, S. G. *Science* **1993**, *260*, 659.

(23) Yi, J.-Y.; Bernholc, J. *Phys. Rev. B: Condens. Matter Mater. Phys.* **1993**, *47*, 1708.

(24) Rubio, A.; Corkill, J. L.; Cohen, M. L. *Phys. Rev. B: Condens. Matter Mater. Phys.* **1994**, *49*, 5081.

(25) Miyamoto, Y.; Rubio, A.; Cohen, M. L.; Louie, S. G. *Phys. Rev. B: Condens. Matter Mater. Phys.* **1994**, *50*, 4976.

(26) Miyamoto, Y.; Rubio, A.; Louie, S. G.; Cohen, M. L. *Phys. Rev. B: Condens. Matter Mater. Phys.* **1994**, *50*, 18360.

(27) Blase, X.; Rubio, A.; Louie, S. G.; Cohen, M. L. *Europhys. Lett.* **1994**, *28*, 335.
(28) Blase, X.; Charlier, J.-C.; De Vita, A.; Car, R. *Appl. Phys. Lett.* **1997**, *70*, 197.
(29) Wang, B.-C.; Tsai, M.-H.; Chou, Y.-M. *Synth. Met.* **1997**, *86*, 2379.
(30) Menon, M.; Srivastava, D. *Chem. Phys. Lett.* **1999**, *307*, 407.
(31) Carroll, D. L.; Redlich, P.; Ajayan, P. M.; Curran, S.; Roth, S.; Rühle, M. *Carbon* **1998**, *36*, 753.
(32) Blase, X.; Charlier, J.-C.; De Vita, A.; Car, R. *Appl. Phys. A: Mater. Sci. Process.* **1999**, *68*, 293.
(33) Fowler, P. W.; Rogers, K. M.; Seifert, G.; Terrones, M.; Terrones, H. *Chem. Phys. Lett.* **1999**, *299*, 359.
(34) Pokropivny, V. V.; Skorokhod, V. V.; Oleinik, G. S.; Kurdyumov, A. V.; Bartnitskaya, T. S.; Pokropivny, A. V. Sisonyuk, A. G. Scheichenko, D. M. J. *Solid State Chem.* **2000**, *154*, 214.
(35) Hirano, T.; Oku, T.; Suganuma, K. *Diamond Relat. Mater.* **2000**, *9*, 625.
(36) Erkoc, S. *THEOCHEM* **2001**, *542*, 89.
(37) Kongsted, J.; Osted, A.; Jensen, L.; Åstrand, P.; Mikkelsen, K. V. *J. Phys. Chem. B* **2001**, *105*, 10243.
(38) (a) Kato, T.; Yamabe, T. *J. Chem. Phys.* **2003**, *118*, 3804. (b) Kato, T.; Yamabe, T. *Recent Research Developments in Quantum Chemistry*; Transworld Research Network: Kerala, 2004.
(39) Albright, T. A.; Burdett, J. K.; Whangbo, M.-H. *Orbital Interactions in Chemistry*; Wiley: New York, 1985.
(40) Conwell, E. M. *Phys. Rev. B: Condens. Matter Mater. Phys.* **1980**, *22*, 1761.
(41) (a) Becke, A. D. *Phys. Rev. A: At., Mol., Opt. Phys.* **1988**, *38*, 3098. (b) *J. Chem. Phys.* **1993**, *98*, 5648.
(42) Lee, C.; Yang, W.; Parr, R. G. *Phys. Rev. B: Condens. Matter Mater. Phys.* **1988**, *37*, 785.
(43) (a) Ditchfield, R.; Hehre, W. J.; Pople, J. A. *J. Chem. Phys.* **1971**, *54*, 724. (b) Hariharan, P. C.; Pople, J. A. *Theor. Chim. Acta* **1973**, *28*, 213.
(44) Frisch, M. J.; Trucks, G. W.; Schlegel, H. B.; Scuseria, G. E.; Robb, M. A.; Cheeseman, J. R.; Zakrzewski, V. G.; Montgomery, J. A.; Stratmann, R. E.; Burant, J. C.; Dapprich, S.; Millam, J. M.; Daniels, A. D.; Kudin, K. N.; Strain, M. C.; Farkas, O.; Tomasi, J.; Barone, V.; Cossi, M.; Cammi, R.; Mennucci, B.; Pomelli, C.; Adamo, C.; Clifford, S.; Ochterski, J.; Paterson, G. A.; Ayala, P. Y.; Cui, Q.; Morokuma, K.; Malick, D. K.; Rabuck, A. D.; Raghavachari, K.; Foresman, J. B.; Cioslowski, J.; Ortiz, J. V.; Stefanov, B. B.; Liu, G.; Liashenko, A.; Piskorz, P.; Komaromi, I.; Gomperts, R.; Martin, R. L.; Fox, D. J.; Keith, T.; Al-Laham, M. A.; Peng, C. Y.; Nanayakkara, A.; Gonzalez, C.; Challacombe, M.; Gill, P. M. W.; Johnson, B. G.; Chen, W.; Wong, M. W.; Andres, J. L.; Head-Gordon, M.; Replogle, E. S.; Pople, J. A.; *Gaussian 98*; Gaussian Inc.: Pittsburgh, PA, 1998.
(45) Allred, A. L. *J. Inorg. Nucl. Chem.* **1961**, *17*, 215.
(46) Kivelson, S.; Heeger, A. J. *Synth. Met.* **1988**, *22*, 371.
(47) Kittel, C. *Quantum Theory of Solids*; Wiley: New York, 1963.